Mathematical models incorporating a multi-stage cell cycle explain synchronisation in proliferation experiments

Sean T. Vittadello[1], Scott W. McCue[1], Gency Gunasingh[2], Nikolas K. Haass[2], Matthew J. Simpson[1,*]

Abstract

We present a suite of experimental data showing that cell proliferation assays, prepared using standard protocols thought to lead to asynchronous populations, persistently exhibit synchronisation. Our experiments use novel fluorescent cell cycle tracking to illustrate synchronisation by highlighting oscillatory subpopulations within the total population of cells. In a more standard setting, without cell cycle tracking, we can only quantify the total cell population and we show that the total cell population data in all our experiments appears to grow exponentially. These observations appear to be conflicting. One potential explanation of these observations is the impact of cell synchronisation, and we show how to reconcile these conflicting observations using a multi-stage model of cell proliferation. Overall, our study has important implications for understanding and improving experimental reproducibility. In summary, while the total population of cells appears to grow exponentially, consistent with an asynchronous population of cells, careful experimental interrogation confirms that standard protocols lead to persistent synchronisation. This normally hidden feature could explain irreproducibility of experiments that examine the role of antimitotic drugs.

Key words and phrases: Cell proliferation, synchronisation, reproducibility, cell cycle, FUCCI, mathematical model

[1] School of Mathematical Sciences, Queensland University of Technology, Brisbane QLD 4001, Australia.

[2] The University of Queensland, The University of Queensland Diamantina Institute, Translational Research Institute, Woolloongabba, Brisbane QLD 4102, Australia.

[*] matthew.simpson@qut.edu.au

1 Introduction

Cell proliferation is essential for many normal and pathological processes. Many different mathematical models of proliferation have been proposed [1–6]. It is often assumed that cells proliferate exponentially,

$$\frac{\mathrm{d}M(t)}{\mathrm{d}t} = \lambda M(t), \quad M(t) = M(0)\mathrm{e}^{\lambda t}, \tag{1}$$

where $M(t)$ is the number of cells at time t and $\lambda > 0$ is the proliferation rate. The eukaryotic cell cycle consists of four phases in sequence from birth to cell division, namely gap 1 (G1), synthesis (S), gap 2 (G2) and mitosis (M) (Figure 1(a)). A key assumption implicit in Equation (1) is that the cell population is asynchronous, meaning that cells are distributed randomly among the cell cycle phases (Figure 1(b)). In contrast, a population of cells is synchronous if the cells are in the same cell cycle phase (Figure 1(c)), or partially synchronous if only a subpopulation of cells is synchronous (Figure 1(d)). Classical exponential growth models, and generalisations thereof [7], implicitly assume the proliferation rate is constant, do not account for subpopulations, and predict monotonic growth. Further, for an exponentially-growing asynchronous population, the per capita growth rate, $(1/M(t))\,\mathrm{d}M(t)/\mathrm{d}t = \lambda$, is constant. In a partially synchronous population, however, synchronous cells divide as a cohort in discrete stages producing a variable per capita growth rate.

Here we provide new experimental data that are inconsistent with Equation (1), and related generalisations, due to the unexpected presence of partially synchronous cell populations. Our data are in the form of two-dimensional proliferation assays. We identify subpopulations based on cell cycle phase by employing fluorescent ubiquitination-based cell cycle indicator (FUCCI) [8]. FUCCI enables visualisation of the cell cycle of individual live cells via two sensors: when the cell is in G1 the nucleus fluoresces red, and when the cell is in S/G2/M the nucleus fluoresces green. During the G1/S transition, early S (eS), both sensors fluoresce and the nucleus appears yellow (Figure 1(a)). Our assays are prepared using a standard method normally thought to achieve asynchronous populations. Over three cell lines and four independent experiments, however, we consistently observe partial synchronisation.

While our total cell population appears to grow exponentially, as expected, neglecting to account for synchronous subpopulations can have important implications for experiment reproducibility. For example,

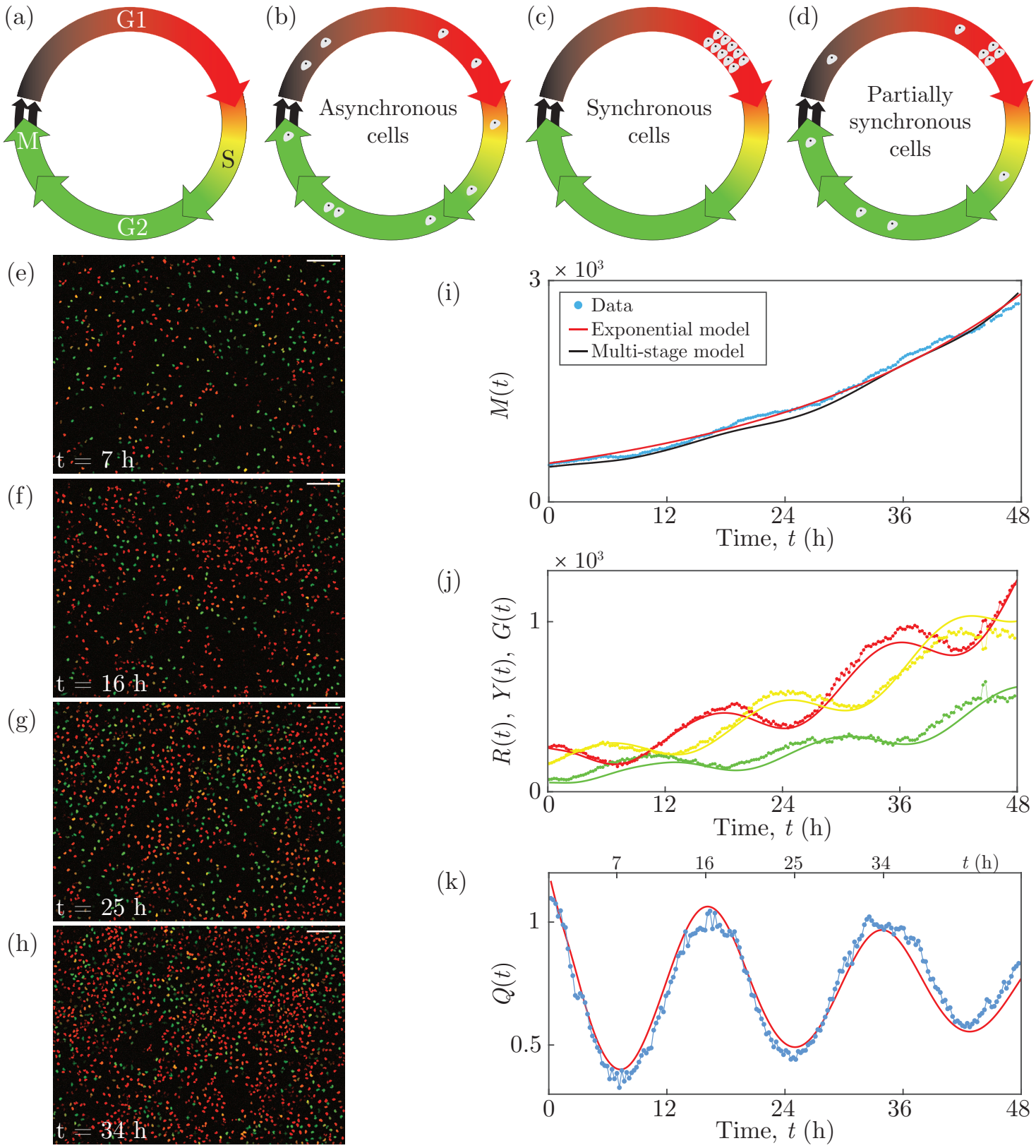

Figure 1: C8161 experimental data and multi-stage model solution. (a) The cell cycle, indicating the colour of FUCCI in each phase. (b)–(d) Asynchronous, synchronous and partially synchronous cells. (e)–(h) Images of a proliferation assay with FUCCI-C8161 cells. Scale bar 200 μm. (i) $M(t)$. (j) $R(t)$, $Y(t)$ and $G(t)$. (k) $Q(t)$. Experimental data are shown as discs and the model solutions as curves.

the correct evaluation of cell cycle phase specific anti-cancer drugs is highly dependent on the cell cycle distribution of the cell population [9]. In a partially synchronous population, the drug may have a delayed or advanced effect compared with an asynchronous population, depending on the cell cycle position of the synchronous cells. Without quantitative techniques such as FUCCI to probe the cell cycle, we have no means of determining whether a population is asynchronous or not in a standard cell proliferation assay. In this standard situation, the assessment of anti-cancer drugs may depend on the timing of application and the nature of the synchronisation, if present. Without quantitative measurements and understanding of these details, such experiments would be difficult or impossible to reproduce.

2 Results

2.1 Experimental data

Our experimental data are time-series images from two-dimensional proliferation assays using melanoma cells. Experiments are performed using three melanoma cell lines C8161, WM983C and 1205Lu [10–12], which have cell cycle times of approximately 18, 27 and 36 h, respectively [10]. Four independent experiments are performed for each cell line. Cells are seeded from subconfluent culture flasks onto a 24-well plate at a density of 10^4 cells cm^{-2}, using 2.5 ml of medium per well. After incubating the plate for 24 h, live-cell images are acquired at 15 minute intervals over 48 h.

Images of a FUCCI-C8161 proliferation assay at 7, 16, 25 and 34 h show red, yellow or green nuclei corresponding to the phases G1, eS or S/G2/M (Figure 1(e)–(h)). The population growth is evident, which we quantify by counting the cells in each image (Supporting Information) to give the number of cells in the total population $M(t)$ at time t (Figure 1(i)). The total number of cells appears to grow exponentially over 48 h, supported by the best fit of Equation (1) (Supporting Information). The numbers of cells in the subpopulations $R(t)$, $Y(t)$ and $G(t)$ with red, yellow or green nuclei (Figure 1(j)), where $M(t) = R(t) + Y(t) + G(t)$, are oscillatory. In an asynchronous population, the subpopulations would exhibit monotone growth. The oscillations we observe here, however, reveal that the cells are partially synchronous.

To explore the synchronisation further, we group cells in the eS and S/G2/M phases together, since eS is

part of S, and consider the ratio $Q(t) = R(t)/\big(Y(t) + G(t)\big)$ (Figure 1(k)). Synchronisation is clearly evident in the oscillatory nature of $Q(t)$. Note the troughs at 7 and 25 h and the peaks at 16 and 34 h are separated by 18 h, which is the approximate cell cycle time for the C8161 cell line. We can visualise the oscillations in these two subpopulations (Figure 1(e)–(h)), where the ratio of the number of red cells to the number of yellow and green cells is lower at 7 and 25 h and higher at 16 and 34 h. Equation (1) and related generalisations are unable to account for the oscillations in these subpopulations. Similar observations are made for two different cell lines (Supporting Information).

2.2 Mathematical model

We employ a multi-stage model of cell proliferation [13] which is capable of describing synchronous populations. The model assumes that the cell cycle times in a population follow a hypoexponential distribution, which consists of a series of independent exponential distributions with different rates. To apply this model we consider partitioning the cell cycle into k stages, P_i, where the duration of each P_i is exponentially distributed with mean μ_i. If $\mathcal{T}$ is the mean cell cycle time then $\sum_{i=1}^{k} \mu_i = \mathcal{T}$. The stages P_i do not necessarily correspond to phases of the cell cycle, however they are mathematically useful to mimic realistic cell cycle times. If we let the transition rates be $\lambda_i = 1/\mu_i$ and consider the partitioned cell cycle $P_1 \xrightarrow{\lambda_1} P_2 \xrightarrow{\lambda_2} \cdots \xrightarrow{\lambda_{k-1}} P_k \xrightarrow{\lambda_k} 2P_1$, we arrive at a system of linear ordinary differential equations describing the mean population $M_i(t)$ in each stage [13]:

$$\frac{\mathrm{d}M_i(t)}{\mathrm{d}t} = \begin{cases} 2\lambda_k M_k(t) - \lambda_1 M_1(t), & \text{for } i = 1, \\ \lambda_{i-1} M_{i-1}(t) - \lambda_i M_i(t), & \text{for } i = 2, \ldots, k. \end{cases} \tag{2}$$

Note that $M(t) = \sum_{i=1}^{k} M_i(t)$. If $k = 1$ then Equation (2) simplifies to Equation (1). During the 48 h time course of our experiments, none of the cell lines exhibit contact inhibition of proliferation, consistent with the typical dysregulation of cell contact inhibition in cancer [14]. Consequently, there is no carrying capacity in the model.

We solve Equation (2) numerically with the forward Euler method, and estimate the parameters by fitting the solution to our experimental data (Supporting Information). $M(t)$ (Figure 1(i)), $R(t)$, $Y(t)$, $G(t)$ (Figure 1(j)) and $Q(t)$ (Figure 1(k)) all correspond well with the experimental data. In particular, the multi-

stage model predicts oscillations in $R(t)$, $Y(t)$, $G(t)$ and $Q(t)$, a feature that is not possible with traditional exponential models.

3 Conclusion

Our new experimental data demonstrate that partially synchronous cell populations may appear to grow exponentially, despite subpopulations exhibiting oscillatory growth. Our experimental set-up observes standard methods thought to produce asynchronous populations; however, all of our proliferation assays exhibit partial synchronisation. We use FUCCI to track cell cycle progression, which is necessary to confirm cell synchronisation. The presence of a partially synchronous population may affect the reproducibility of experiments, an observation which may contribute towards an explanation for reproducibility issues with experiments involving cell cycle specific anti-cancer drugs. As the standard exponential growth model cannot account for subpopulations with oscillating growth, we successfully utilise a multi-stage model of cell proliferation to describe oscillations in population growth.

4 Author Contributions

All authors designed the research. STV performed the research. All authors contributed analytic tools and analysed the data. STV wrote the manuscript, and all authors approved the final version of the manuscript.

5 Acknowledgments

NKH is a Cameron fellow of the Melanoma and Skin Cancer Research Institute, and is supported by the NHMRC (AP1084893). MJS is supported by the ARC (DP170100474).

References

[1] Sherratt JA, Murray JD. Models of epidermal wound healing. Proc R Soc B. 1990;241:29–36.

[2] Swanson KR, Bridge C, Murray JD, Alvord EC. Virtual and real brain tumors: using mathematical modeling to quantify glioma growth and invasion. J Neurol Sci. 2003;216:1–10.

[3] Maini PK, McElwain DLS, Leavesley DI. Traveling wave model to interpret a wound-healing cell migration assay for human peritoneal mesothelial cells. Tissue Eng. 2004;10:475–482.

[4] Scott JG, Basanta D, Anderson ARA, Gerlee P. A mathematical model of tumour self-seeding reveals secondary metastatic deposits as drivers of primary tumour growth. J R Soc Interface. 2013;10:20130011.

[5] Sarapata EA, de Pillis LG. A comparison and catalog of intrinsic tumor growth models. Bull Math Biol. 2014;76:2010–2024.

[6] Böttcher MA, Dingli D, Werner B, Traulsen A. Replicative cellular age distributions in compartmentalized tissues. J R Soc Interface. 2018;15:20180272.

[7] Tsoularis A, Wallace J. Analysis of logistic growth models. Math Biosci. 2002;179:21–55.

[8] Sakaue-Sawano A, Kurokawa H, Morimura T, Hanyu A, Hama H, Osawa H, et al. Visualizing spatiotemporal dynamics of multicellular cell-cycle progression. Cell. 2008;132:487–498.

[9] Beaumont KA, Hill DS, Daignault SM, Lui GYL, Sharp DM, Gabrielli B, et al. Cell cycle phase-specific drug resistance as an escape mechanism of melanoma cells. J Invest Dermatol. 2016;136:1479–1489.

[10] Haass NK, Beaumont KA, Hill DS, Anfosso A, Mrass P, Munoz MA, et al. Real-time cell cycle imaging during melanoma growth, invasion, and drug response. Pigment Cell Melanoma Res. 2014;27:764–776.

[11] Vittadello ST, McCue SW, Gunasingh G, Haass NK, Simpson MJ. Mathematical models for cell migration with real-time cell cycle dynamics. Biophys J. 2018;114:1241–1253.

[12] Simpson MJ, Jin W, Vittadello ST, Tambyah TA, Ryan JM, Gunasingh G, et al. Stochastic models of cell invasion with fluorescent cell cycle indicators. Physica A. 2018;510:375–386.

[13] Yates CA, Ford MJ, Mort RL. A multi-stage representation of cell proliferation as a Markov process. Bull Math Biol. 2017;79(12):2905–2928.

[14] Hanahan D, Weinberg RA. Hallmarks of cancer: The next generation. Cell. 2011;144(5):646–674.